Membrane topology of the Na+/citrate transporter CitS of Klebsiella pneumoniae by insertion mutagenesis

Geest, Marleen van; Lolkema, Juke S.

Published in:
Biochimica et Biophysica Acta-Biomembranes

DOI:
10.1016/S0005-2736(00)00185-1

Publication date:
2000

ELSEVIER

Biochimica et Biophysica Acta 1466 (2000) 328–338

BIOCHIMICA ET BIOPHYSICA ACTA
BBA

www.elsevier.com/locate/bba

Membrane topology of the Na^+/citrate transporter CitS of *Klebsiella pneumoniae* by insertion mutagenesis

Marleen van Geest, Juke S. Lolkema *

Department of Microbiology, Groningen Biomolecular Sciences and Biotechnology Institute, University of Groningen, Kerklaan 30, 9751 NN Haren, The Netherlands

Received 12 October 1999; received in revised form 17 February 2000; accepted 2 March 2000

Abstract

The sodium ion dependent citrate transporter of *Klebsiella pneumoniae* (CitS) is a member of the bacterial 2-hydroxycarboxylate transporter family. Membrane topology models of the protein, largely based on reporter molecule fusions to C-terminally truncated CitS molecules, indicate that the protein traverses the membrane 11 times with the NH_2-terminus in the cytoplasm and the COOH-terminus in the periplasm. Furthermore, the structure is characterized by unusual long loops in the COOH-terminal half of the protein: one hydrophobic segment between transmembrane segments V and VI in the periplasm and three long loops connecting transmembrane segments VI and VII, VIII and IX and X and XI in the cytoplasm. The 10 kDa biotin acceptor domain and six consecutive His residues (His-tag) were inserted at different positions in the four long loops and the effect on transport activity and protein stability was analyzed. Six out of seven insertion mutants were stably expressed and three of these had retained significant transport activity. The sidedness of the tags in the mutants that tolerated the insertion was determined by proteolysis experiments. The results support the 11 transmembrane segment model that was based upon truncated CitS proteins.

Keywords: Membrane topology; Insertion mutagenesis; Citrate transport; His-tag; Biotin acceptor domain

1. Introduction

In *Klebsiella pneumoniae* a unique Na^+ dependent citrate transporter (CitS) is induced upon anaerobic growth on citrate [1,2]. Transport of citrate catalyzed by CitS is strictly coupled to the uptake of two Na^+ ions and is driven by an electrochemical gradient of Na^+ ions [3–5]. The *citS* gene is part of an operon that contains the genes for the enzymes of the anaerobic citrate degradation pathway in *K. pneumoniae*, the transporter CitS, citrate lyase and the primary Na^+ pump, oxaloacetate decarboxylase [6]. The amino acid sequence of CitS revealed that the protein is a member of the bacterial 2-hydroxycarboxylate transporter (2HCT) family [6]. CitS is the most distant member in the family with close to 30% sequence identity with the citrate and malate transporters of the Gram-positive lactic acid bacteria and two transporters of unknown function in *Bacillus subtilis*.

The membrane topology of CitS has been studied in the *Escherichia coli* membrane by a combination of alkaline phosphatase (PhoA) fusions, biotin acceptor domain (BAD) fusions to the NH_2- and COOH-

* Corresponding author. Fax: +31-50-3632154; E-mail: j.s.lolkema@biol.rug.nl

0005-2736/00/$ – see front matter
PII: S0005-2736(00)00185-1

termini, and site directed Cys labelling of the loop between segments VIII and IX [7,8]. The folding of CitS was studied also in the endoplasmic reticulum membrane using in vitro translation/insertion of C-terminally truncated CitS molecules engineered in place of the second transmembrane segment (TMS) of the *E. coli* membrane protein leader peptidase [9]. The model for the membrane topology obtained for CitS was found to be the same in the two types of membranes, but different from the 12 transmembrane helix structure common to most secondary transporters which was also the predicted model for CitS (Fig. 1A). In the experimental model, the CitS protein traverses the membrane 11 times with the NH_2-terminus in the cytoplasm and the COOH-terminus in the periplasm and contains a number of long loops in the COOH-terminal half of the protein (Fig. 1C). A strongly conserved hydrophobic stretch of about 25 amino acid residues (segment Vb) that was predicted to be transmembrane is situated in the periplasm between TMSs V and VI. Three other long loops are cytoplasmic, between TMSs VI and VII, VIII and IX, and X and XI. The most COOH-terminal loop between TMSs X and XI is the second highly conserved region in the 2HCT family and, even though the amino acid residues in the other two loops are not, the length of the loops is well conserved.

The topology model of CitS is based largely upon C-terminal deletion mutants and, therefore, it is assumed that the folding of the C-terminally truncated proteins does not depend on C-terminal sequences. The assumption was falsified for fusions of PhoA to sites in the loop between TMSs VIII and IX that resulted in a periplasmic location of the PhoA molecule (Fig. 1B). Site directed Cys labelling of cysteine residues engineered in the same loop clearly demonstrated that in the complete protein the loop is in the cytoplasm [8]. In the present study another approach was taken to bypass potential problems with the fusion approach to confirm the membrane topology of the C-terminal half of the protein. Tags were inserted in the four extended loops of the CitS protein and their sidedness was determined by proteolysis experiments. Several positions in the loops were found

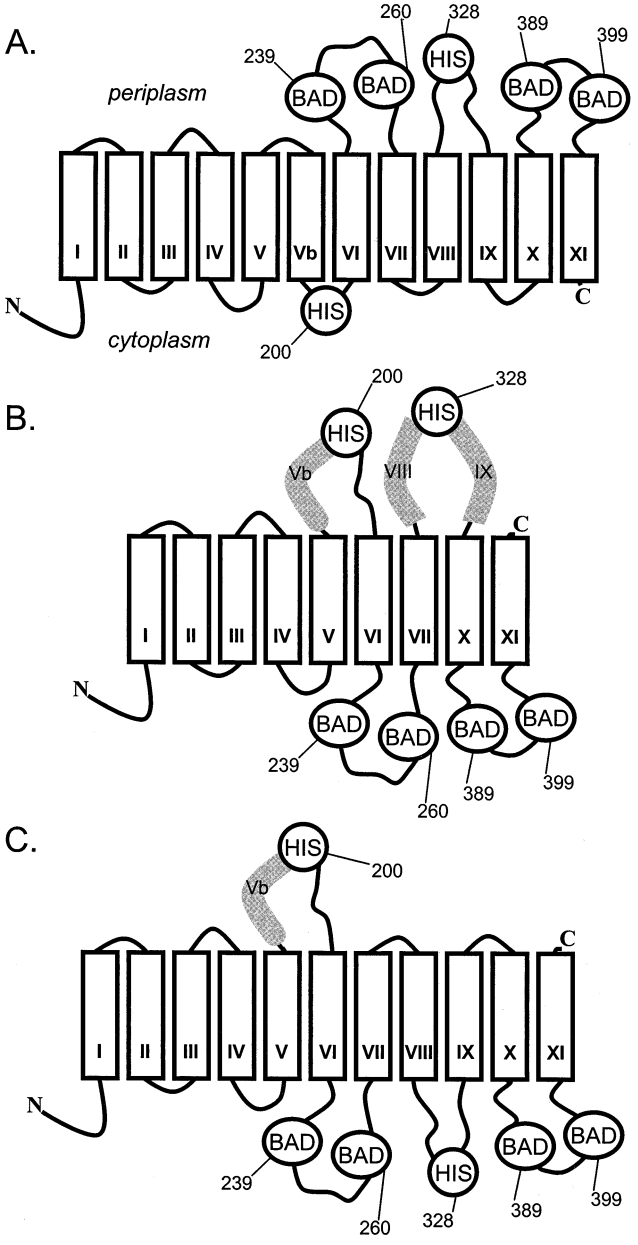

Fig. 1. Membrane topology models of CitS. (A) Predicted model based on the hydropathy profile of the amino acid sequence [7,9]. (B) Model based on C-terminal deletion PhoA fusions [7]. (C) Model based on a combination of PhoA fusions and single Cys labelling [8,9]. Putative transmembrane segments are depicted as boxes and the lengths of the connecting loops are roughly in accord with the number of residues in the loops. Numbers indicate the position of amino acid residues. Gray shaded loop regions represent hydrophobic stretches that were predicted to be transmembrane. Sites for insertion of the BAD and His-tag are depicted as circles marked 'BAD' and 'HIS', respectively. The numbering of the transmembrane segments is according to the model in C.

which tolerated the insertion of the 10 kDa BAD of the oxaloacetate decarboxylase of *K. pneumoniae* or a sequence of six histidine residues (His-tag). These engineered transporters showed transport activity, indicating that the critical parts of the CitS moiety are folded as in the native CitS protein. The results were in agreement with the folding model of CitS depicted in Fig. 1C.

2. Materials and methods

2.1. Materials

Ni^{2+}-NTA resin was obtained from Qiagen, alkaline phosphatase (AP) labelled streptavidin from Boehringer Mannheim, monoclonal antibodies against AP and against the His-tag from Chemicon International (Temecula, CA, USA) and Dianova (Hamburg, Germany), respectively. Oligonucleotides were obtained from Eurosequence (Groningen, The Netherlands). The amino acid sequence of CitS is available in the SwissProt database under accession number P31602 and the Transport Protein Classification number is TC 2.24.1.1.

2.2. Bacterial strains and growth conditions

E. coli strain BL21(DE3) was routinely grown in Luria broth (LB) medium at 37°C. Expression of CitS derivatives cloned in the vector pBluescript II SK (Stratagene, La Jolla, CA, USA) was obtained without induction. Carbenicillin was added at a final concentration of 100 μg/ml. Citrate transport activity in the recombinant strains was detected as blue colonies on Simmons citrate agar plates (Difco). AP activity was detected as blue colonies on LB agar plates containing the chromogenic substrate 5-bromo-4-chloro-3-indolyl-phosphate (toluidine salt; XP) at a concentration of 40 μg/ml.

2.3. Genetic manipulations

Standard recombinant DNA procedures were used essentially as described by Sambrook et al. [10]. All the fragments obtained by PCR were sequenced after subcloning using an Amersham automated sequencer.

2.3.1. Construction of BAD insertion mutants pSBxxx

Unique *Nco*I sites (CCATGG) were introduced throughout the *citS* gene in plasmid pSKΔLCitS [7] by site directed mutagenesis [11] which resulted in a series of CitS-*Nco*I mutants described in [7] and designated pSNxxx, in which xxx refers to the residue number of the methionine residue encoded by the ATG codon in the introduced *Nco*I site. A PCR fragment encoding the BAD of the oxaloacetate decarboxylase of *K. pneumoniae* with *Nco*I sites in the flanking regions [7] was ligated into the *Nco*I sites of pSN239, pSN260, pSN328, pSN389 and pSN399 yielding plasmids pSB239, pSB260, pSB328, pSB389 and pSB399, respectively.

2.3.2. Construction of His insertion mutants, pSHxxx

Two complementary oligonucleotides (5′-CATG-**CATCACCATCACCATCAC**GG-3′, 5′-CATGCC**GTGATGGTGATGGTGATG**-3′) were mixed and phosphorylated in a mixture containing 5 μl of each primer (10 μM), 2 μl ATP (10 mM), 2 μl polynucleotide kinase, 2 μl 10×kinase buffer and 4 μl H_2O. The mixture was incubated at 37°C for 1 h followed by an incubation at 65°C for 20 min. The resulting stretch of double stranded DNA encoded six histidine residues (bold; His-linker) and contained at either end an overhang compatible with an *Nco*I site. Subsequently, the His-linker was ligated into the *Nco*I sites of pSN200 and pSN328 yielding pSH200 and pSH328. Insertion of the linker destroyed the *Nco*I site, which was used to screen for positive clones. The correct orientation of the inserted His-tag and the reading frame were analyzed by DNA sequencing.

2.3.3. Construction of PhoA fusions

To assay for the expression of a number of CitS derivatives, the gene encoding mature AP was fused at the 3′ end of the *citS* gene. Plasmid pSA445, encoding CitS with the C-terminus fused to the mature part of PhoA [7], was used to make these constructs. A unique *Pst*I site in the *citS* gene is located 160 bp upstream of the 3′ end and a unique *Sac*I site is located in the multiple cloning site downstream of the *citS* or *phoA* genes. The *Pst*I–*Sac*I fragment of pSA445 was isolated and ligated into pSN328, pSB328, pSH328, pSN389 and pSB389 restricted

with *Pst*I and *Sac*I, resulting in pSN328A, pSB328A, pSH328A, pSN389A, and pSB389A, respectively.

2.4. Biochemical techniques

2.4.1. SDS–PAGE and immunoblot analysis

Cells were resuspended to an OD_{600} of 10, diluted with a one-fifth volume of loading buffer and boiled for 3 min after which 5 μl samples were loaded onto sodium dodecyl sulfate (SDS)–polyacrylamide gels containing 10 or 12.5% polyacrylamide. After electrophoresis, the proteins were transferred to Immobilon-P membranes (Millipore) by semidry electrophoretic blotting. PhoA fusion proteins were detected with monoclonal antibodies directed against PhoA, His-tagged proteins were detected with monoclonal anti-His-tag antibodies and biotinylated proteins were detected with AP labelled streptavidin, all at a dilution of 1:5000. Antibodies and streptavidin were visualized using the Western-light chemiluminescence detection kit with CSPD as a substrate as recommended by the manufacturer (Tropix).

2.4.2. Preparation of ISO membranes and spheroplasts

Cells were grown to an OD_{600} of 1, harvested and washed once with 50 mM potassium phosphate pH 7, 100 mM NaCl. Inside-out (ISO) membranes were prepared by resuspending the cells in the same buffer containing 1 mM EDTA, 1 mM $MgSO_4$ and a trace amount of deoxyribonuclease. Cells were broken by one passage through a French press cell operated at 10 000 psi at 4°C and immediately mixed with a phenylmethylsulfonyl fluoride (PMSF) solution yielding a final concentration of 1 mM. Unbroken cells and debris were removed by centrifugation at $14\,000\times g$ for 10 min at 4°C, and the ISO membranes were collected from the supernatant by ultracentrifugation at $100\,000\times g$ for 30 min. Membranes were washed once in 50 mM potassium phosphate pH 7 and stored in liquid nitrogen. Spheroplasts were prepared essentially as described by Herzlinger et al. [12] with modifications as described in [7]. Briefly, cells harvested at an OD_{600} of 0.5 were resuspended in 10 mM Tris–HCl pH 8, 0.75 M sucrose to an OD_{600} of 10 and incubated for 10 min. Lysozyme solution was added to a final concentration of 25 μg/ml followed by an additional 10 min of incubation. The suspension was diluted three-fold in a solution containing 1.5 mM K-EDTA and 10 mg/ml lysozyme and incubated for 1 h at 4°C. The spheroplasts were harvested by centrifugation in a tabletop centrifuge and washed once in 100 mM potassium phosphate pH 7, 0.5 M sucrose and concentrated five times in the same buffer. The spheroplasts were used immediately for the proteolytic experiments.

2.4.3. Proteinase K treatment

Proteinase K was added to ISO membranes or to spheroplasts using a freshly prepared stock solution of 10 mg/ml. Incubation of 0.2–0.5 mg/ml ISO membranes or the spheroplasts with 0.4 mg/ml proteinase K was performed on ice and stopped after 1 h by adding PMSF to a final concentration of 1 mM. When indicated Triton X-100 was added at 2% concentration to the ISO membranes or spheroplasts prior to the addition of proteinase K. The intactness of the spheroplasts after proteinase K treatment was inferred from the presence of a 22 kDa band after immunoblotting using AP labelled streptavidin. The 22 kDa band corresponds to acetyl-CoA carboxylase, the only endogenous biotinylated protein of *E. coli*.

2.4.4. Ni^{2+}-NTA purification procedure

ISO membranes (4 mg/ml) of His-tagged CitS derivatives were solubilized in 50 mM potassium phosphate pH 8, 400 mM NaCl, 20% glycerol and 1% Triton X-100. The solution was left on ice for 1 h with intermittent agitation. Undissolved material was removed by ultracentrifugation at $80\,000\times g$ for 20 min at 4°C. The supernatant was mixed with Ni^{2+}-NTA resin (100 μl per 10 mg of protein) equilibrated in 50 mM potassium phosphate pH 8, 300 mM NaCl, 10% glycerol, 0.1% Triton X-100 and 20 mM imidazole and incubated for 2.5 h at 4°C under continuous shaking and, subsequently, poured into a column. The column was washed with 2 ml equilibration buffer and, subsequently, with 1 ml equilibration buffer containing 30 mM imidazole. The protein was eluted with 2×250 μl of the same buffer containing 200 mM imidazole. The eluate was mixed with loading buffer and loaded on a 10% SDS–polyacrylamide gel that was used for immunoblotting or stained with silver.

3. Results

3.1. Activity and expression of NcoI mutants

In a previous study [7] a series of *Nco*I mutants of CitS (SNxxx) were constructed that were used to construct CitS–PhoA fusions. For the present study we selected the mutants with the *Nco*I sites in the regions of the *citS* gene encoding the long loops in the C-terminal half of the protein. Table 1 lists the *Nco*I mutants, together with the mutations in the translated amino acid sequences. Expression of CitS in *E. coli* results in citrate uptake and metabolism as is evident from the appearance of blue halos around colonies on Simmons agar indicator plates. Wild-type *E. coli* cells exhibit a negative phenotype on these indicator plates because of the lack of a citrate uptake system. The ability of the *Nco*I mutants to transport citrate was tested on the Simmons agar plates. Only one of the mutants, SN328, resulted in a negative phenotype, indicative of an inactive citrate transport protein or lack of expression of the mutant protein. Expression of SN328 was measured by fusing the mature part of PhoA as a tag to the C-terminus, yielding SN328A. The C-terminal PhoA fusion of wild-type CitS (SN445A) was used as a control [7]. Immunoblotting using antibodies against PhoA showed a band at an apparent mass of 83 kDa corresponding to the full length CitS–PhoA fusion proteins, both for SN328A and for the control (Fig. 2A) (see also [7]). A plate assay using indicator plates to measure PhoA activity demonstrated high PhoA activity for cells expressing SN328A, indicating a periplasmic location of the C-terminus as is the case for the wild-type CitS protein. These observations show that CitS mutant SN328 is expressed, but is not active. We will use the PhoA fusion assay to determine the expression of inactive CitS derivatives throughout this paper.

3.2. CitS–BAD insertion mutants

The N- and C-terminal *Nco*I mutants, SN1 and SN445, respectively, are active and it was shown before that fusion of the BAD of the α-subunit of the oxaloacetate decarboxylase of *K. pneumoniae* to either terminus does not affect activity. In vivo biotinylation of the CitS–BAD fusion proteins by biotin ligase was demonstrated using AP labelled streptavidin [7]. A previous study with the lactose transporter LacY of *E. coli* showed that the BAD could only successfully be inserted in cytoplasmic loops of the protein. BAD inserted in periplasmic domains remained at the cytoplasmic face of the membrane, resulting in misfolded, inactive proteins [13]. Therefore, in our search for catalytically active insertion mutants, we decided to insert the BAD only in the putative cytoplasmic loops of CitS. The BAD gene was inserted in the *Nco*I site of the mutants SN239, SN260, SN328, SN389 and SN399 resulting in SB239, SB260, SB328, SB389 and SB399, respectively. The resulting proteins have the BAD inserted in the cytoplasmic loops between putative TMSs VI and VII, TMSs VIII and IX and TMSs X and IX.

Table 1
Properties of CitS SNxxx mutants

Site(xxx)	Loop	*Nco*I mutations (SNxxx)		BAD insertions (SBxxx)		His-tag insertions (SHxxx)
		Mutation	Activity[b]	Activity[b]	Biotinylation	Activity[b]
1[a]	N_t	T2S	+	+	+	+
200	V/VI	V200M,T201A	+	nd[c]	nd	+
239	VI/VII	W239M,L240V	+	−	+	nd
260	VI/VII	K259T,T260M	+	+	+	nd
328	VIII/IX	R327P,L328M,S329A	−	−	−	−
389	X/XI	I389M	+	+	−	nd
399	X/XI	C398S	+	−	+	nd
445[a]	C_t	M444T,I446V	+	+	+	+

[a]Data from [7] and added for completeness.
[b]Positive phenotype on Simmons agar indicator plates.
[c]Not done; these insertions were not constructed.

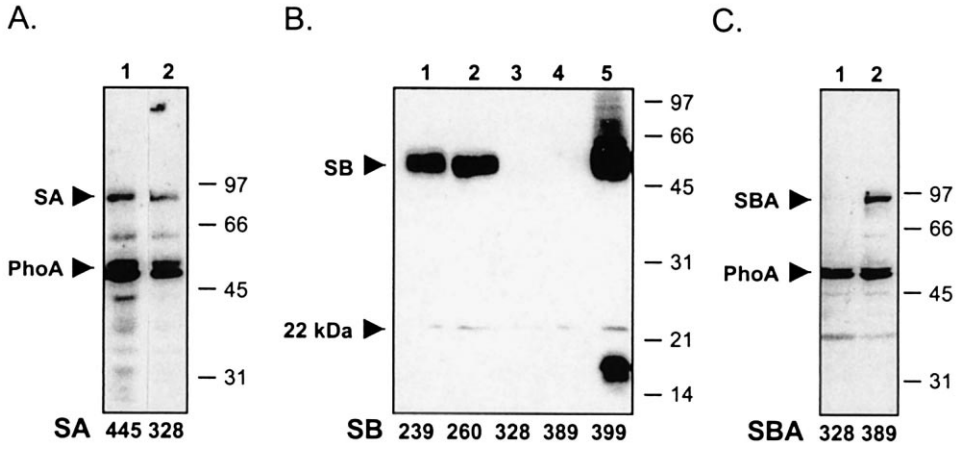

Fig. 2. Western blot analysis of CitS–BAD insertion mutants. Cells expressing CitS derivatives were analyzed for alkaline phosphatase using antibodies raised against PhoA (A, C) and biotinylation using AP labelled streptavidin (B). (A) CitS–PhoA fusions SA445 (lane 1) and SN328A (lane 2). (B) CitS–BAD insertion mutants SB239, SB260, SB328, SB389, and SB399 (lanes 1–5, respectively). (C) CitS–BAD–PhoA insertion/fusion proteins SB328A (lane 1) and SB389A (lane 2). The arrows indicate CitS–PhoA fusion proteins (SA), mature PhoA (PhoA), CitS–BAD insertion proteins (SB), CitS–BAD–PhoA insertion–fusion proteins (SBA) and acetyl-CoA carboxylase (22 kDa). Indicated at the side of the panels are the positions of the molecular size markers.

Insertion of the BAD in the loop between segments VI and VII at position 260 resulted in an active CitS moiety, while insertion in the same loop but at position 239 was not tolerated (Table 1). As expected, insertion mutant SB328 which has the BAD inserted in the *Nco*I site of the inactive SN328 mutant, between TMSs VIII and IX, resulted in a negative phenotype on the indicator plates. Insertion of the BAD in the loop between segments X and XI resulted in CitS activity when the BAD was inserted at position 389 while no activity could be detected when it was inserted at position 399.

Expression and in vivo biotinylation of the insertion mutants was analyzed by Western blotting of whole cell extracts using AP labelled streptavidin (Fig. 2B). *E. coli* contains one endogenous biotinylated protein, acetyl-CoA carboxylase, which results in a 22 kDa band in all lanes. Cells expressing SB239, SB260 and SB399 showed a strong additional band with an apparent mass of 48 kDa (Fig. 2B, lanes 1, 2, and 5), demonstrating that the CitS–BAD insertion mutants were synthesized and biotinylated in vivo. The size of the insertion mutants was the same as observed for the CitS–BAD fusion proteins SB1 and SB445 [7]. No biotinylated CitS proteins were detected in cells expressing SB328 and SB389. The level of expression of SB328 and SB389 was analyzed by fusing PhoA to the C-terminus of both derivatives resulting in the tripartite proteins SB328A and SB389A. Consistent with the observed CitS activity of SB389, immunoblotting of cells expressing SB389A revealed a band with a molecular mass of 93 kDa in agreement with the size of the CitS–BAD–PhoA molecule (Fig. 2C, lane 2). Apparently, the BAD moiety of the protein is not biotinylated in vivo by biotin ligase. No fusion protein was observed in the case of SB328A, suggesting that insertion of the BAD at position 328 in CitS results in unstable molecules that are rapidly degraded (Fig. 2C, lane 1).

In summary, insertion of the BAD in the loop between TMSs VI and VII resulted in in vivo biotinylated CitS that was active when the insertion was at position 260 and inactive at position 239. Insertion in the loop between TMSs X and XI resulted in CitS that was active but not biotinylated when the insertion was at position 389 and biotinylated but not active when the insertion was at position 399. Insertion of the BAD at position 328, between TMSs VIII and IX, resulted in degradation of the protein (Table 1).

3.3. Sidedness of the BAD in SB260 and SB399

The active CitS–BAD fusions SB1 and SB445 allowed the localization of the N- and C-termini of

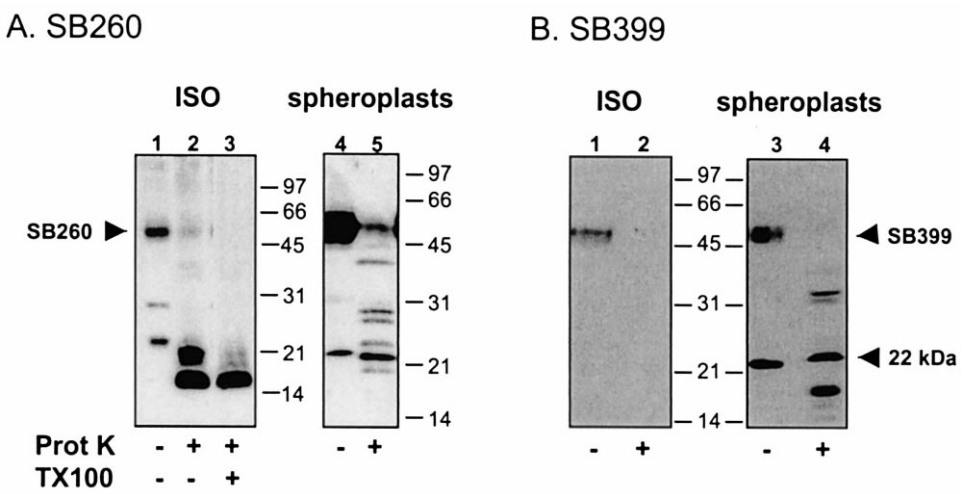

Fig. 3. Proteinase K digestion of SB260 (A) and SB399 (B). ISO membranes and spheroplasts prepared from *E. coli* BL21 (DE3) cells expressing CitS–BAD insertion mutants SB260 and SB399 were treated with (+) and without (−) proteinase K (Prot K) and in the presence (+) and absence (−) of Triton X-100 (TX100) as indicated. Biotinylated proteins were detected with AP labelled streptavidin. Arrows labelled SB260 and SB399 indicate the full length insertion mutants. The arrow labelled 22 kDa indicates the acetyl-CoA carboxylase of *E. coli*. Indicated at the side of the panels are the positions of the molecular size markers.

CitS in the cytoplasm and periplasm, respectively, by proteolysis experiments [7]. The localization of the BAD in the CitS–BAD insertion mutants with the BAD in the loops between segments VI and VII (SB260) and X and XI (SB399) was determined similarly by exposing each chimera in ISO membranes and in spheroplasts to proteinase K. When ISO membranes containing SB260 were treated with proteinase K, a loss of the full length protein was observed along with the appearance of two low molecular weight bands of approximately 15 and 20 kDa (Fig. 3A, lanes 1 and 2). In time, the 20 kDa band was converted into the 15 kDa band that was stable upon prolonged treatment. Proteinase K treatment of the same ISO membranes in the presence of 2% Triton X-100 resulted in a similar pattern with a somewhat faster interconversion of the two bands (Fig. 3A, lane 3). Apparently, the 15 kDa band is resistant to proteinase K. A similar proteinase K resistant fragment was not observed when the BAD was fused to the N- and C-termini of CitS [7] and when BAD was inserted at position 399 (see below), suggesting that the BAD in SB260 is protected by flanking CitS sequences. At any rate, the BAD in SB260 is accessible from the cytoplasmic side of the membrane. In the complementary experiment, treatment of spheroplasts containing SB260 led to the appearance of multiple cleavage products, (Fig. 3A, lanes 4 and 5) suggesting that the BAD itself is not accessible for proteinase K at the periplasmic side, but that the CitS part is cleaved in periplasmic loops. In the presence of 2% Triton X-100, exposure to proteinase K resulted in the 15 kDa band, as expected (not shown). Together, the results imply that the BAD in SB260, which is active in citrate transport, is inserted in a cytoplasmic domain, in agreement with the model in Fig. 1C. Similar experiments were performed with spheroplasts of cells expressing SB239 that was not active. The same cleavage products were observed as with SB260 which is consistent with the localization of the BAD in one and the same cytoplasmic loop (results not shown).

Proteinase K treatment of ISO membranes containing SB399 with the BAD inserted in the loop between TMSs X and XI resulted in the complete loss of the full length fusion protein (Fig. 3B, lanes 1 and 2) and no degradation products were detected, indicating that the BAD is accessible for proteinase K from the cytoplasmic side of the membrane. In agreement with this conclusion, when spheroplasts containing SB399 were exposed to proteinase K, stable cleavage products appeared, indicating that the BAD itself is protected by the membrane for cleavage (Fig. 3B, lanes 3 and 4). In SB399 (inactive) the

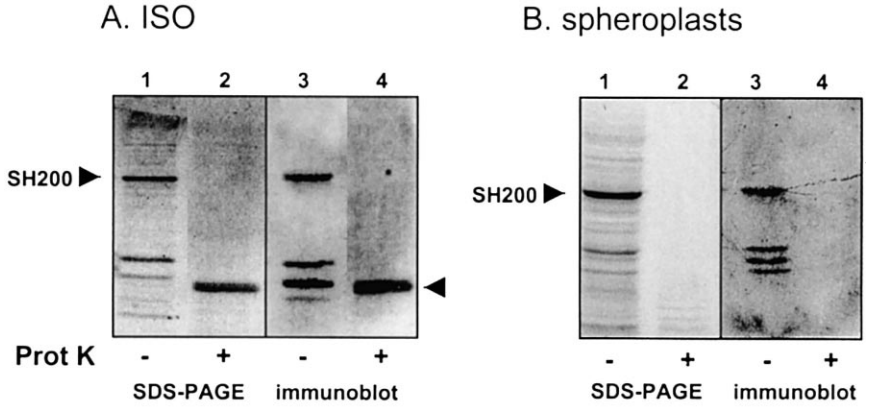

Fig. 4. Proteinase K digestion of SH200. ISO membranes (A) and spheroplasts (B) from cells expressing His-tag insertion mutant SH200 were incubated with (+) and without (−) proteinase K. After treatment, His-tagged proteins were partially purified by Ni^{2+}-NTA chromatography and analyzed by silver stained SDS–PAGE (lanes 1 and 2) and by immunoblotting using monoclonal antibodies directed against the His-tag (lanes 3 and 4). The full length His-tagged CitS protein and the cleaved product (A, lanes 2 and 4) are indicated by arrows.

BAD is inserted in a cytoplasmic domain, consistent with the topology model in Fig. 1C.

3.4. CitS–His-tag insertion mutants

A His-tag, consisting of six consecutive histidine residues, was inserted in mutant SN200 containing the *Nco*I site in the periplasmic loop between TMSs V and VI and in SN328 containing the *Nco*I site in the loop between TMSs VIII and IX that did not accept the BAD insertion. Insertion of the His-tag at position 200 (mutant SH200), at the end of the hydrophobic stretch Vb, resulted in active CitS molecules (Table 1). The protein could be partially purified in a single step by Ni^{2+}-NTA affinity chromatography and detected as a band with an apparent molecular weight of 38 kDa by SDS–PAGE which is in agreement with the molecular mass of similar constructs reported before (Fig. 4A,B, lanes 1)[4]. The 38 kDa band showed reactivity with antibodies raised against the His-tag (Fig. 4A,B, lanes 3). Some of the impurities in the preparation represent breakdown products as is evident from the lower molecular weight bands in the immunoblots. The cellular localization of the His-tag in SH200 was determined as described above. Proteinase K treatment of ISO membranes resulted in the complete loss of the 38 kDa band, while a new band with a lower molecular weight appeared (Fig. 4A, lane 2). The presence of the His-tag at the latter protein fragment was demonstrated by immunoblotting (lane 4). Apparently, the His-tag itself is not accessible, but the CitS protein is cleaved in one or more cytoplasmic loops. Consistent with this view is the complete loss of any His-tagged protein when spheroplasts were treated with proteinase K (Fig. 4B, lanes 2 and 4), indicating that the His-tag is susceptible to cleavage at the periplasmic side of the membrane. Together the results clearly demonstrate that the His-tag in active mutant SH200 has a periplasmic location, consistent with the topology model based upon truncated CitS molecules.

Cells expressing SH328, with the His-tag inserted between segments VIII and IX, resulted in a very faint band at the expected position after purification (results not shown). In contrast to what was observed with the BAD inserted at the same position, labelling of the SH328 protein at the C-terminus with PhoA, yielding SH328A, revealed good expression and a periplasmic location of the C-terminus (not shown). Apparently, the His-tag at position 328 is not accessible to the Ni^{2+}-NTA resin.

4. Discussion

The CitS protein is believed to span the membrane 11 times with the NH_2-terminus in the cytoplasm

and the COOH-terminus in the periplasm. The model was obtained from studies in *E. coli* as well as in dog pancreas microsomes using truncated CitS molecules fused in front of a topological reporter molecule [7,9]. A disadvantage of the fusion technique is that the folding of the CitS part in the fusion protein may be different from the folding of the same part in the complete CitS molecule. This was evident from PhoA fusions at sites in the loop between TMSs VIII and IX that resulted in periplasmic PhoA, thereby erroneously reporting the localization in the complete protein (Fig. 1B). The correct localization was determined by site directed Cys labelling techniques [8]. In the present study tags were inserted in loops of CitS and their sidedness with respect to the membrane supports certain aspects of the model in Fig. 1C. The sidedness of the tags was determined for those insertion mutants that tolerated the insertion by showing citrate transport activity (SH200, SB260) or, at least, resulted in a stable CitS derivative (SB399). Moreover, in the latter construct, a C-terminal PhoA fusion of SB399 showed that the C-terminus was correctly located in the periplasm (not shown). It is assumed that the structure of CitS is not severely disrupted in these constructs. Proteolytic experiments with constructs in which a His-tag was inserted in the periplasmic loop between segments V and VI (SH200) and the BAD inserted in the loop between segments VI and VII (SB260) confirmed the periplasmic and cytoplasmic location of the loops, respectively. Similarly, the cytoplasmic location of the loop in between segments X and XI was confirmed in construct SB399. A CitS molecule with the BAD inserted 10 residues upstream at position 389 (SB389) showed citrate transport activity, indicating correct folding of the CitS moiety. Insertion of the BAD in periplasmic domains of LacY of *E. coli* was shown to result in misfolded, inactive transporter molecules [13]. Therefore, it is likely that the BAD in SB389 is in a cytoplasmic domain and that the lack of in vivo biotinylation is due to the inaccessibility of the biotinylation site to the biotin ligase.

The common architecture of bacterial secondary transporters is a bundle of transmembrane α-helices that are connected by, usually, short hydrophilic loops. The hydrophilic loops in a membrane protein may be very flexible with their main function being to connect the TMSs. Such a view is supported by the insertions of His-tags and the BAD in many loops of the lactose transport protein LacY that result in a protein active in proton motive force driven lactose transport [13,14]. On the other hand, mutations in the loops of the same protein and other transporters have been described that affect the substrate specificity or activity of the transporters, suggesting a role for loop regions in catalysis and a defined structure of the loop [15–18]. The CitS molecule contains four loops that are considerably longer than usually observed in bacterial secondary transporters, a feature that is conserved throughout the 2HCT family. It is likely that these loops play some role in the structure and/or function of the transporter. Insertion of the 10 kDa BAD was accepted at four out of five tested positions in these loop regions, while the His-tag could be inserted in both tested positions without destabilizing the molecule. Only half of the six stable insertion mutants had retained citrate transport activity.

The periplasmic loop between TMSs V and VI is about 40 residues long and contains hydrophobic stretch Vb that was originally predicted to be transmembrane (see Fig. 1) [7]. The stretch contains nine conserved residues, including four Gly and two Pro, and is one of the two most conserved regions of the 2HCT family. A His-tag could be inserted just downstream of the segment without loss of activity (Table 1, SH200) and the tagged protein could be purified by Ni^{2+}-NTA affinity chromatography, indicating that the inserted His-tag is exposed to the water phase. The data suggest that the region downstream of the conserved stretch is a flexible loop structure.

The cytoplasmic loop between TMSs VI and VII is about 30 residues long of which only two are conserved (two Gly). The loop resembles somewhat the large cytoplasmic loop that separates the NH_2- and COOH-terminal halves of the transporters of the major facilitator superfamily even though there is no evidence for structural similarity between transporters of the two families [19]. The 10 kDa BAD was inserted in the COOH-terminus (SB260) and the NH_2-terminus (SB239). Insertion at both positions resulted in a stable and in vivo biotinylated chimera, suggesting that the structure was not severely disturbed. Remarkably, the insertion at position 239 inactivated the protein, while the chimera with the BAD inserted at position 260 was active in citrate

transport. It appears that the relevance of a loop for catalysis cannot be evaluated from a single insertion in the loop.

The loop between TMSs VIII and IX is about 25 residues long, contains no conserved residues and is only moderately hydrophilic. We noted before that the loop is strongly amphipathic when folded as an α-helix [9], a feature that is conserved throughout the members of the family. Possibly, this region forms a surface helix, exposing its hydrophobic face towards the membrane and its hydrophilic face towards the cytoplasm. In SN328, three residues in the putative amphipathic helix are mutated, which leaves the protein stable, but completely inactivates it (Table 1). Insertion of the 10 kDa BAD at this position resulted in rapid degradation of the protein, while insertion of the much smaller His-tag left the protein stable. The His-tagged protein could not be purified by Ni^{2+}-NTA affinity chromatography, suggesting that the tag is folded in the structure of CitS. The data suggest that the loop between TMSs VIII and IX is very well structured and important to the function of CitS.

The most COOH-terminal cytoplasmic loop of CitS is about 45 residues long and contains the second well conserved region of the 2HCT family just in front of TMS XI with seven and nine out of 21 identical and similar residues, respectively. Insertion of the BAD at position 398, just in front of the conserved region, inactivated the protein, but the protein was stably expressed and biotinylated in vivo. Insertion of the BAD 10 residues upstream in SB389 did not inactivate the protein, but the BAD could not be biotinylated in vivo, suggesting that the domain, at least in part, was buried in the structure of the loop.

Acknowledgements

The authors wish to thank W.N. Konings for critically reading the manuscript and for many helpful discussions.

References

[1] P. Dimroth, A. Thomer, Citrate transport in *Klebsiella pneumoniae*, Biol. Chem. Hoppe-Seyler 367 (1986) 813–823.

[2] M.E. van der Rest, R.M. Siewe, T. Abee, E. Schwarz, D. Oesterhelt, W.N. Konings, Nucleotide sequence and functional properties of a sodium-dependent citrate transport system from *Klebsiella pneumoniae*, J. Biol. Chem. 267 (1992) 8971–8976.

[3] J.S. Lolkema, H. Enequist, M.E. van der Rest, Transport of citrate catalyzed by the sodium-dependent citrate carrier of *Klebsiella pneumoniae* is obligatorily coupled to the transport of two sodium ions, Eur. J. Biochem. 220 (1994) 469–475.

[4] K.M. Pos, M. Bott, P. Dimroth, Purification of two active fusion proteins of the Na^+-dependent citrate carrier of *Klebsiella pneumoniae*, FEBS Lett. 347 (1994) 37–41.

[5] K.M. Pos, P. Dimroth, Functional properties of the purified Na^+-dependent citrate carrier of *Klebsiella pneumoniae*: evidence for asymmetric orientation of the carrier protein in proteoliposomes, Biochemistry 35 (1996) 1018–1026.

[6] M. Bott, M. Meyer, P. Dimroth, Regulation of anaerobic citrate metabolism in *Klebsiella pneumoniae*, Mol. Microbiol. 18 (1995) 533–546.

[7] M. van Geest, J.S. Lolkema, Membrane topology of the sodium ion-dependent citrate carrier of *Klebsiella pneumoniae*. Evidence for a new structural class of secondary transporters, J. Biol. Chem. 271 (1996) 25582–25589.

[8] M. van Geest, J.S. Lolkema, TMS VIII of the Na^+/citrate transporter CitS requires downstream TMS IX for insertion in the *Escherichia coli* membrane, J. Biol. Chem. 274 (1999) 29705–29711.

[9] M. van Geest, I. Nilsson, G. von Heijne, J.S. Lolkema, Insertion of a bacterial secondary transport protein in the endoplasmic reticulum membrane, J. Biol. Chem. 274 (1999) 2816–2823.

[10] J. Sambrook, E.F. Fritsch, T. Maniatis, Molecular Cloning: A Laboratory Manual, 2nd edn., Cold Spring Harbor laboratory, Cold Spring Harbor, NY, 1989.

[11] T. Kunkel, J.D. Roberts, R.A. Zakour, Methods Enzymol. 154 (1987) 367–386.

[12] D. Herzlinger, P. Viitanen, N. Carrasco, H.R. Kaback, Monoclonal antibodies against the lac carrier protein from *Escherichia coli*. 2. Binding studies with membrane vesicles and proteoliposomes reconstituted with purified lac carrier protein, Biochemistry 23 (1984) 3688–3693.

[13] K.H. Zen, T.G. Consler, H.R. Kaback, Insertion of the polytopic membrane protein lactose permease occurs by multiple mechanisms, Biochemistry 34 (1995) 3430–3437.

[14] E. McKenna, D. Hardy, H.R. Kaback, Insertional mutagenesis of hydrophilic domains in the lactose permease of *Escherichia coli*, Proc. Natl. Acad. Sci. USA 89 (1992) 11954–11958.

[15] S. Frillingos, M. Sahin-Toth, J. Wu, H.R. Kaback, Cys-scanning mutagenesis: a novel approach to structure function relationships in polytopic membrane proteins, FASEB J. 12 (1998) 1281–1299.

[16] N.J. Pazdernik, A.E. Jessen-Marshall, R.J. Brooker, Role of conserved residues in hydrophilic loop 8–9 of the lactose permease, J. Bacteriol. 179 (1997) 735–741.

[17] B. Poolman, J. Knol, C. van der Does, P.J. Henderson, W.J. Liang, G. Leblanc, T. Pourcher, I. Mus-Veteau, Cation and sugar selectivity determinants in a novel family of transport proteins, Mol. Microbiol. 19 (1996) 911–922.
[18] L.A. Hu, S.C. King, Membrane topology of the *Escherichia coli* gamma-aminobutyrate transporter: implications on the topography and mechanism of prokaryotic and eukaryotic transporters from the APC superfamily, Biochem. J. 336 (1998) 69–76.
[19] J.S. Lolkema, D.J. Slotboom, Estimation of structural similarity of membrane proteins by hydropathy profile alignment, Mol. Membr. Biol. 15 (1998) 33–42.